Stem Cell Reports
Article

ISSCR

OPEN ACCESS

Regulation of male germline transmission patterns by the Trp53-Cdkn1a pathway

Mito Kanatsu-Shinohara,[1,2] Honda Naoki,[3] Takashi Tanaka,[1] Misako Tatehana,[4] Takako Kikkawa,[4] Noriko Osumi,[4] and Takashi Shinohara[1,*]

[1]Department of Molecular Genetics, Graduate School of Medicine, Kyoto University, Kyoto 606-8501, Japan
[2]AMED-CREST, Chiyodaku, Tokyo 100-0004, Japan
[3]Laboratory of Data-driven Biology, Graduate School of Integrated Sciences for Life, Hiroshima University, Higashi-Hiroshima, Hiroshima, Japan
[4]Department of Developmental Neuroscience, United Centers for Advanced Research and Translational Medicine (ART), Tohoku University Graduate School of Medicine, Sendai, Japan
*Correspondence: tshinoha@virus.kyoto-u.ac.jp
https://doi.org/10.1016/j.stemcr.2022.07.007

SUMMARY

A small number of offspring are born from the numerous sperm generated from spermatogonial stem cells (SSCs). However, little is known regarding the rules and molecular mechanisms that govern germline transmission patterns. Here we report that the *Trp53* tumor suppressor gene limits germline genetic diversity via *Cdkn1a*. *Trp53*-deficient SSCs outcompeted wild-type (WT) SSCs and produced significantly more progeny after co-transplantation into infertile mice. Lentivirus-mediated transgenerational lineage analysis showed that offspring bearing the same virus integration were repeatedly born in a non-random pattern from WT SSCs. However, SSCs lacking *Trp53* or *Cdkn1a* sired transgenic offspring in random patterns with increased genetic diversity. Apoptosis of KIT^+ differentiating germ cells was reduced in *Trp53*- or *Cdkn1a*-deficient mice. Reduced CDKN1A expression in *Trp53*-deficient spermatogonia suggested that *Cdkn1a* limits genetic diversity by supporting apoptosis of syncytial spermatogonial clones. Therefore, the TRP53-CDKN1A pathway regulates tumorigenesis and the germline transmission pattern.

INTRODUCTION

Spermatogenesis depends on continuous self-renewal division of spermatogonial stem cells (SSCs) (Meistrich and van Beek, 1993; de Rooij, 2017). Upon differentiation, clones of spermatogonia undergo mitotic expansion on the basement membranes of seminiferous tubules. Nine to eleven cell divisions of spermatogonia and two divisions of spermatocytes build the germ cell population of the testis. In rats, one SSC is estimated to produce 4,096 sperm via self-renewal division (Russell et al., 1990). The first morphological indication of spermatogonial differentiation is incomplete cytokinesis, which results in generation of germ cell clones connected by intercellular cytoplasmic bridges. As they differentiate, these clones gradually transmigrate through the blood-testis barrier between Sertoli cells while undergoing meiosis before maturation into spermatozoa (Smith and Braun, 2012). Although the number of SSCs varies depending on the method of evaluation, functional transplantation assays have shown that approximately 150–3,000 SSCs are present in the testis (Oatley et al., 2011; Kanatsu-Shinohara et al., 2016; Boyer et al., 2021). These cells are presumed to undergo constant division and contribute equally to fertilization. However, the number of offspring born in a litter is limited, and typical litter size varies from 5.2 to 7.0 in mice (Silver, 1995). Therefore, only a limited number of SSCs can fertilize eggs and transmit genetic information despite production of a large number of sperm throughout life. However, the factors that influence the germline transmission patterns from a pool of SSCs are unknown.

Clonal analysis of spermatogenesis has been hampered by a lack of appropriate techniques. The low frequency and poor transfection efficiency of undifferentiated spermatogonia, which divide only once every 10–13 days (de Rooij, 2017), have been major obstacles. However, we recently developed a method for SSC lineage analysis by clonal marking of SSCs using lentivirus vectors (Kanatsu-Shinohara et al., 2016). After dissociation of testis cells into single cells, testis cells were infected with a virus vector and then transplanted into the seminiferous tubules of infertile mice. These recipient males were subsequently mated with wild-type (WT) females to produce offspring; the offspring DNA was analyzed to determine integration of the virus transgene. Using this procedure, approximately 30%–50% of the offspring contained the transgene. Because only one set of the chromosomes is transmitted to the next generation via meiosis, the results suggested that more than 60% of the SSCs are labeled by this procedure. A unique characteristic of this SSC-based transgenesis is the diverse genetic repertoire. Because individual SSCs are transfected with a retro/lentivirus, single recipient males can produce a large number of transgenic offspring with different transgene integration patterns; indeed, up to 126 patterns could be generated from a single recipient in our study (Kanatsu-Shinohara et al., 2016). By continuously monitoring the transgene integration patterns during the lifetime of recipient males, this method allows transgenerational lineage analysis of SSC clones.

Using this strategy, we previously evaluated the germline transmission patterns of SSCs by monitoring the recipient mice for more than 2 years. The most surprising result from this study was that offspring bearing the same virus integration patterns were frequently born in the same or next litter, which suggested that only a specific SSC clone contributes to produce offspring in a particular litter. This phenomenon of "clustering" was unexpected because more than 5×10^7 spermatozoa are ejaculated in mice for successful fertilization (Harper, 1982). A similar observation was made originally in ethylnitrosourea-induced mouse mutagenesis (Russell et al., 1979); mutants with the same mutation patterns are often born in the same litters. Based on this observation, we designed an experiment to monitor the germline transmission patterns of specific SSC clones in a total of 1,325 offspring derived from spermatogonial transplantation to determine the SSC kinetics. The result suggested that not all SSCs contribute equally to sperm production. Clones that appear only once are not completely lost from the SSC pool; they reappeared later with a mean lifespan of approximately 124.4 days (Kanatsu-Shinohara et al., 2016).

Although the mechanism of this clustering and reappearance phenomenon has not yet been determined, quantitative analysis of cell numbers at differentiation points revealed significant loss of progenitor cells at the differentiating germ cell stage. Morphological studies have shown that approximately 25% of spermatogonia can survive during spermatogenesis (Huckins, 1978). Indeed, the highest number of cells reported to be present in a particular clone is 98 (22 spermatocytes and 76 spermatids) (Russell et al., 1990). Therefore, it is possible that germ cells undergo some kind of selection during spermatogenesis. However, the biological significance and its mechanism have long remained unknown. When we tried to confirm these results by using doxycycline-inducible expression of H2B-GFP fusion lineage tracing, we found that the actual ratio of KIT^+ differentiating germ cells to $CDH1^+$ undifferentiated spermatogonia was approximately 5-fold (Kanatsu-Shinohara et al., 2016). Therefore, the efficiency of spermatogenesis was significantly lower than theoretically estimated. Because germ cells that are connected by intercellular bridges undergo clonal apoptosis (Hamer et al., 2003), we proposed that apoptosis of spermatogonia clones is responsible for the reduced pattern formation.

The purpose of the current study was to identify genes involved in the male germline transmission pattern. We hypothesized that fertile mutant mice with abnormal histology may exhibit abnormal germline transmission patterns. Based on this assumption, we focused on the *Fmr1* and *Trp53* genes. *Fmr1* is responsible for mental retardation; *Fmr1* knockout (KO) mice exhibit macroorchidism, and its expression is found in spermatogonia (Devys et al., 1993; Bakker et al., 1994). In the adult, testis size is mainly a reflection of the number of germ cells present. Therefore, *Fmr1* may be involved in spermatogonial number regulation (Bächner et al., 1993). The expression of *Fmr1* is influenced by an unstable and expanding trinucleotide CGG repeat located in the 5′ untranslated region of *Fmr1*. In contrast, *Trp53* KO mice do not show macroorchidism, but they contain giant spermatogonia and an increased number of sperm with morphological abnormalities (Beumer et al., 1998). We assessed the spermatogonial dynamics by labeling SSCs and then analyzed germline transmission patterns by continuous breeding and evaluation of virus integration patterns in a total of 1,037 offspring derived from WT and mutant SSC transplantation.

RESULTS

Trp53 KO SSCs outcompete WT SSCs after competitive spermatogonial transplantation

To determine the expression patterns of FMR1 and TRP53 in spermatogenic cells, we evaluated the compositions of germ cells in WT mice using antibodies against spermatogonia markers, including GFRA1 (a marker for A_{single} [A_s], A_{paired}, and a portion of $A_{aligned}$ undifferentiated spermatogonia), KIT (a marker for differentiating spermatogonia and early spermatocytes), and SYCP3 (a marker for spermatocytes). The specificity of the antibodies for FMR1 and TRP53 were confirmed by immunostaining or western blot analysis of KO mice (Figures S1A and S1B). Double immunostaining of WT testes showed that FMR1 and TRP53 were widely expressed in the testis (Figures 1A and 1B). Both genes were strongly expressed in cells on the basement membrane. Quantification of signals revealed that only a small proportion of $GFRA1^+$ undifferentiated spermatogonia expressed these genes. However, their expression levels significantly peaked in KIT^+ differentiating germ cells; this was followed by downregulation in $SYCP3^+$ spermatocytes (Figure 1B). Although the expression patterns of FMR1 and TRP53 were comparable in $GFRA1^+$ spermatogonia, FMR1 was expressed more widely in later stages of spermatogenesis. Cytoplasmic localization of FMR1 was consistent with a previous study (Devys et al., 1993). Despite their wide expression patterns, histological analysis of *Fmr1* KO and *Trp53* KO testes showed complete spermatogenesis, and mature spermatozoa were found (Figure 1C).

To test whether these mutant mice exhibited abnormal germline transmission patterns, equal numbers of mutant cells and WT cells were mixed and microinjected into the seminiferous tubules of immature WBB6F1-W/W^v (W) mice (Figure 1D); these mice are congenitally infertile because of mutations in the *Kit* tyrosine kinase gene

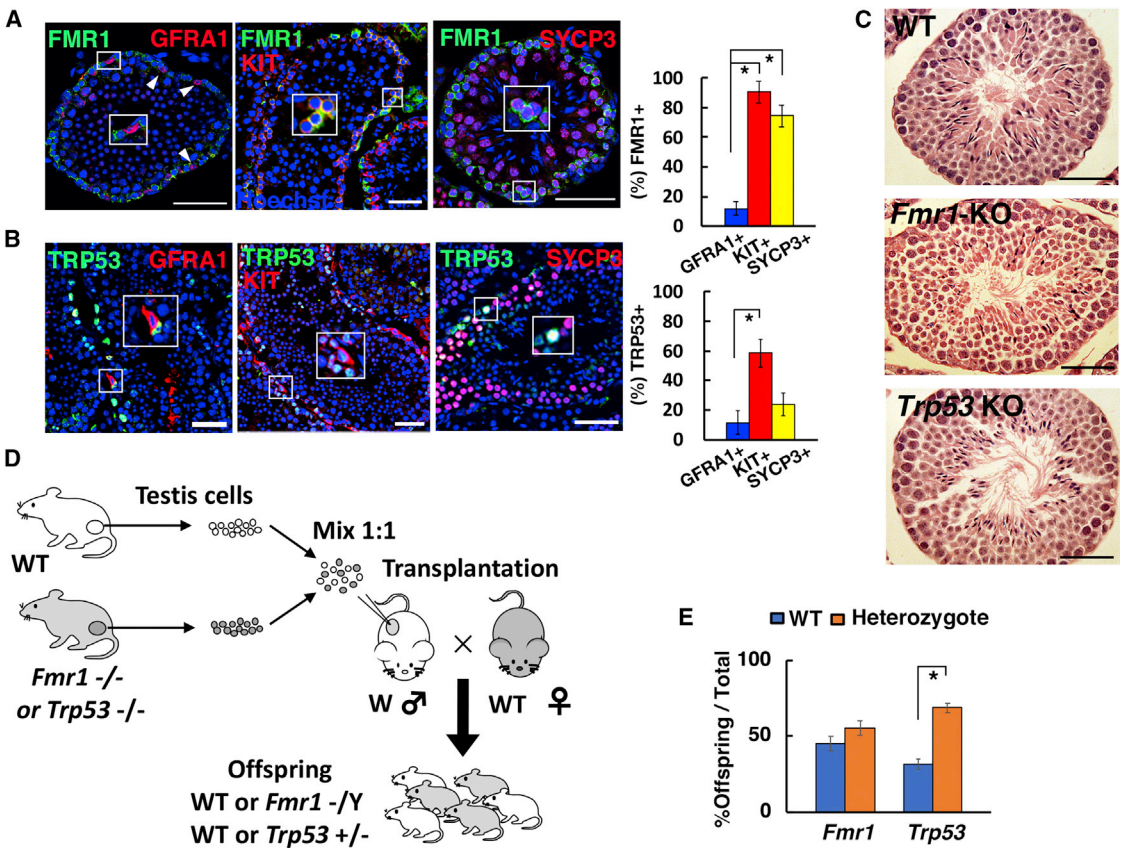

Figure 1. Competitive spermatogonial transplantation

(A and B) Double immunostaining and quantification of FMR1 (A) and TRP53 (B) with spermatogenesis markers in WT testes (n = 12–13 for FMR1, n = 13–15 for TRP53).

(C) Histological appearance of *Fmr1* KO and *Trp53* KO testes.

(D) Experimental schematic showing the competitive spermatogonial transplantation.

(E) Proportion of heterozygous offspring from all recipient mice (n = 31 for *Fmr1*, n = 44 for *Trp53*).

Scale bars, 50 μm (A–C). Counterstain, Hoechst 33342 (A and B) and hematoxylin and eosin (C). Asterisks indicate statistical significance (*p < 0.05). See also Figures S1 and S2 and Tables S2 and S3. Results are means ± SEM.

(Fleischman, 1993). When these recipient mice had matured, they were caged with WT female mice to produce progeny at least 4 weeks after transplantation. Because W mice lack endogenous spermatogenesis, all offspring produced from the recipients must be derived from transplanted donor cells. Two experiments were performed involving *Fmr1* KO mice, and three experiments were performed involving *Trp53* KO mice.

Within 4 months, all recipient males that had received *Fmr1* KO and *Trp53* KO cells sired offspring with mutant alleles (Figures S2A and S2B). Offspring from *Fmr1* KO cells were born as early as 84 days after transplantation. In total, 283 offspring in 31 litters were born from four fertile mice during the 201-day experimental period (Figure S2A). Because *Fmr1* is on the X chromosome (Bakker et al., 1994), all male offspring were WT mice. Therefore, we checked the contributions of WT and *Fmr1* KO SSCs by genotyping female mice. Among 145 female offspring, the *Fmr1* mutant allele was found in 80 mice, whereas 65 mice were born from WT donors. The percentage of offspring with the *Fmr1* mutant allele ranged from 52.4%–57.4% from each recipient. This did not significantly differ from the WT allele, and no statistical difference was found. These results showed that loss of *Fmr1* does not influence germline transmission efficiency.

Trp53 KO SSCs also sired progeny as early as 72 days after transplantation. In total, 293 offspring were born from seven recipients during the 382-day experimental period. Although two of the recipients sired only one litter, one recipient sired as many as 15 litters. No apparent abnormalities were found in the offspring. Polymerase chain reaction (PCR) analysis of tail DNA from offspring revealed that offspring with the *Trp53* mutant allele comprised 195 of 293 (66.6%) total offspring. Offspring with the

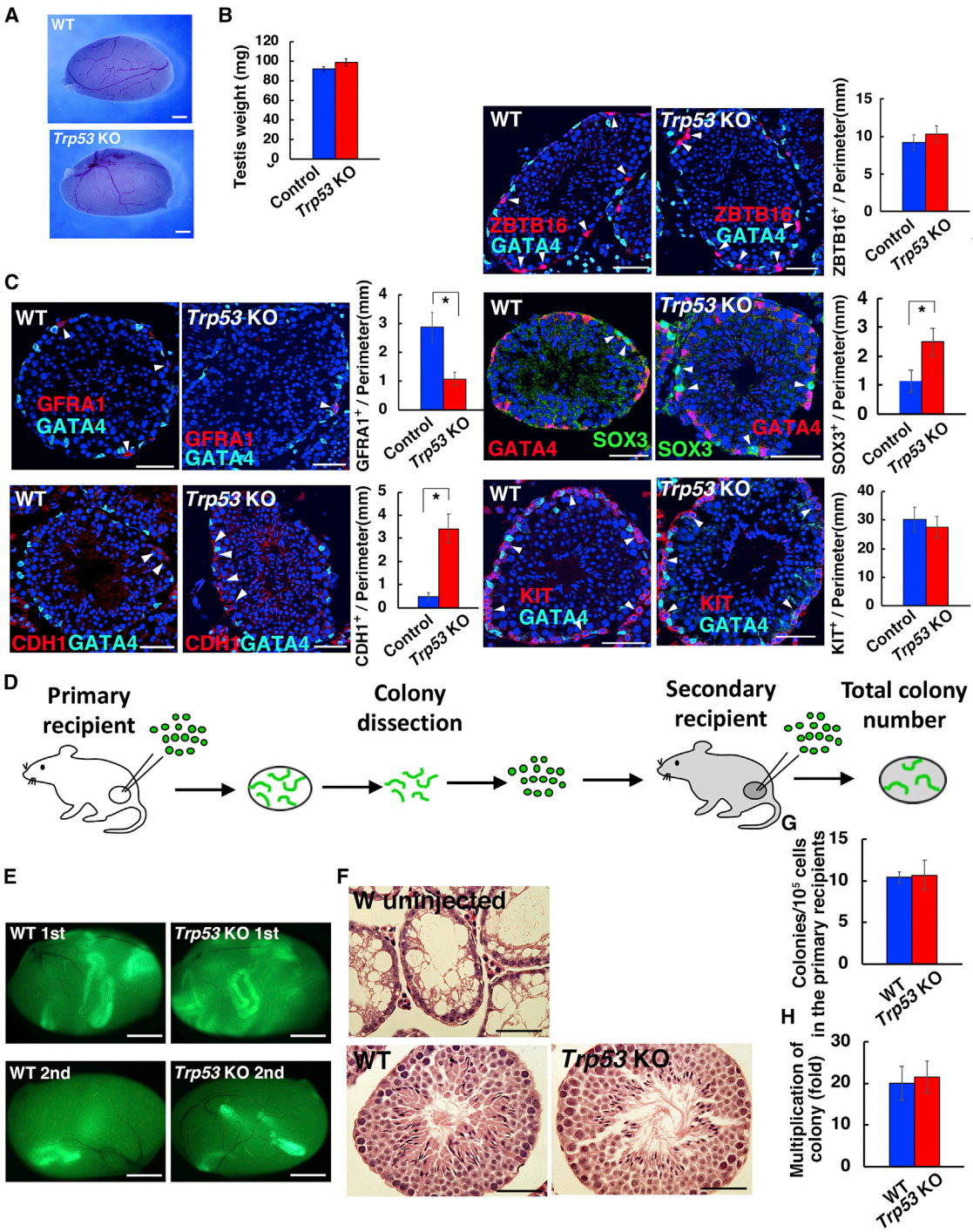

Figure 2. Functional analysis of *Trp53* KO SSCs by serial transplantation

(A) Macroscopic appearance of *Trp53* KO testis.

(B) Testis weight (n = 4).

(C) Double immunostaining of *Trp53* KO testis using antibodies against GATA4 (a Sertoli cell marker) and spermatogonia markers (n = 39–44 for GFRA1, n = 21–23 for ZBTB16, n = 56 for CDH1, n = 49 for SOX3, n = 31–35 for KIT).

(D) Experimental schematic showing serial transplantation.

(E) Macroscopic appearance of recipient testis.

(F) Histological analysis of recipient testis.

(legend continued on next page)

mutant allele were found more frequently in all seven fertile recipient mice (Figure S2B). The percentage of offspring with the *Trp53* mutant allele ranged from 60.0%–72.2%. The difference between *Trp53* and WT alleles was statistically significant (Figure 1E). In nine of 44 litters from four recipient mice, all offspring consisted of mice with the *Trp53* mutant allele. However, such biased contribution was not found for the WT allele. These results suggest that *Trp53* KO SSCs undergo germline transmission more efficiently than WT SSCs despite reported spermatogenic abnormalities.

Serial transplantation of Trp53 KO SSCs

Increased offspring production from *Trp53* KO mice suggested that more mutant spermatozoa were generated from SSCs. We presumed that *Trp53* deficiency enhanced SSC self-renewal because *Trp53* restricts the self-renewal division of several tissue stem cells (Bonizzi et al., 2012). The appearance and size of *Trp53* KO testes did differ from the appearance and size of WT testes (Figures 2A and 2B). We first performed immunostaining to characterize spermatogonium populations in *Trp53* KO testes (Figure 2C). Although we did not find changes in the numbers of $ZBTB16^+$ total undifferentiated spermatogonia and KIT^+ differentiating germ cells, the number of $GFRA1^+$ spermatogonia was significantly reduced in their testes (Figure 2C). This result is consistent with the recent observation that *Trp53*-deficient cultured SSCs exhibit lower levels of *Gfra1* mRNA (Liu et al., 2022), which suggested that this downregulation of *Gfra1* is caused by autonomous action of *Trp53* in germ cells. Because conflicting reports exist regarding GFRA1 expression on SSCs (Buageaw et al., 2005; Ebata et al., 2005; Hara et al., 2014), we also stained CDH1, another SSC marker validated by transplantation assay (Tokuda et al., 2007). In contrast to GFRA1, the number of CDH1 undifferentiated spermatogonia was significantly increased in *Trp53* KO testes. Because this result suggested a relative increase in committed spermatogonia in the undifferentiated spermatogonium population, we stained SOX3, a marker for committed spermatogonia (McAninch et al., 2020). As expected, the number of $SOX3^+$ undifferentiated spermatogonia was significantly increased in *Trp53* KO testes (Figure 2C).

Although these results suggest that *Trp53* KO testes contain a smaller number of SSCs, SSCs are defined only by their function. To quantify SSCs, we carried out spermatogonial transplantation assays (Figure 2D). *Trp53* KO mice were crossed with green mice to introduce a donor cell marker. We transplanted an equal number of testis cells from *Trp53* KO or WT cells into different W recipient mice. Two months after transplantation, the recipient mice were sacrificed, and the germ cell colonies were counted under UV fluorescence (Figure 2E). Histological sections showed complete spermatogenesis after transplantation (Figure 2F). The numbers of colonies generated by *Trp53* KO and WT cells were 10.7 and 10.4 per 10^5 transplanted cells, respectively (Figure 2G). The difference between *Trp53* KO and WT cells was not statistically significant.

Because this result suggested that the concentrations of SSCs in the total cell suspension were comparable between *Trp53* KO and control testes, we dissociated colonies in the primary recipient testes into single cells and then transplanted a portion of the dissociated cells into the secondary recipients to evaluate their self-renewal activity. This allowed us to quantify the number of SSCs that underwent self-renewal division in the primary recipients. Assuming that only 10% of SSCs can colonize the seminiferous tubules and that single SSCs produce spermatogenic colonies (Nagano et al., 1999; Kanatsu-Shinohara et al., 2006), the numbers of secondary colonies generated by primary colonies were 21.5 and 20.1 by *Trp53* KO and control testis cells, respectively (Figure 2H). No significant differences were found between *Trp53* KO and WT mice. Therefore, we concluded that SSC number and self-renewal activity are unchanged by *Trp53* deficiency, which agrees with a previous study that suggested no significant effect of *Trp53* in A_s spermatogonia (Beumer et al., 1998).

Reduced apoptosis of differentiating germ cells in Trp53 KO mice

The lack of apparent defects in SSCs suggests that abnormalities in progenitor cells are responsible for enhanced germline transmission. Therefore, we evaluated the levels of proliferation and apoptosis in *Trp53* KO testes. Although double immunostaining using MKI67 and spermatogonia markers did not show significant differences (Figure S3A), Tdt (terminal deoxynucleotidyl transferase)-mediated dUTP (deoxy-uracil) nick end labeling (TUNEL) staining revealed significantly reduced apoptosis of $ZBTB16^+$ and KIT^+ spermatogonia in *Trp53* KO mice (Figure 3A). We also analyzed spermatocytes and haploid cells by SYCP3 (a spermatocyte marker) and PNA (peanut agglutinin) (a haploid cell marker) staining. However, no differences were evident in the numbers and distribution patterns of these markers

(G) Number of colonies in the primary recipients (n = 9 for *Trp53* KO, n = 10 for WT).
(H) Multiplication of colony numbers ([total regenerated colony number] × 10/primary colony number used for serial transplantation) (n = 9).
Scale bars, 1 mm (A and E) and 50 μm (C and F). Counterstain, Hoechst 33342 (C) and hematoxylin and eosin (F). Asterisks indicate statistical significance (*p < 0.05). See also Figure S3 and Table S2. Results are means ± SEM.

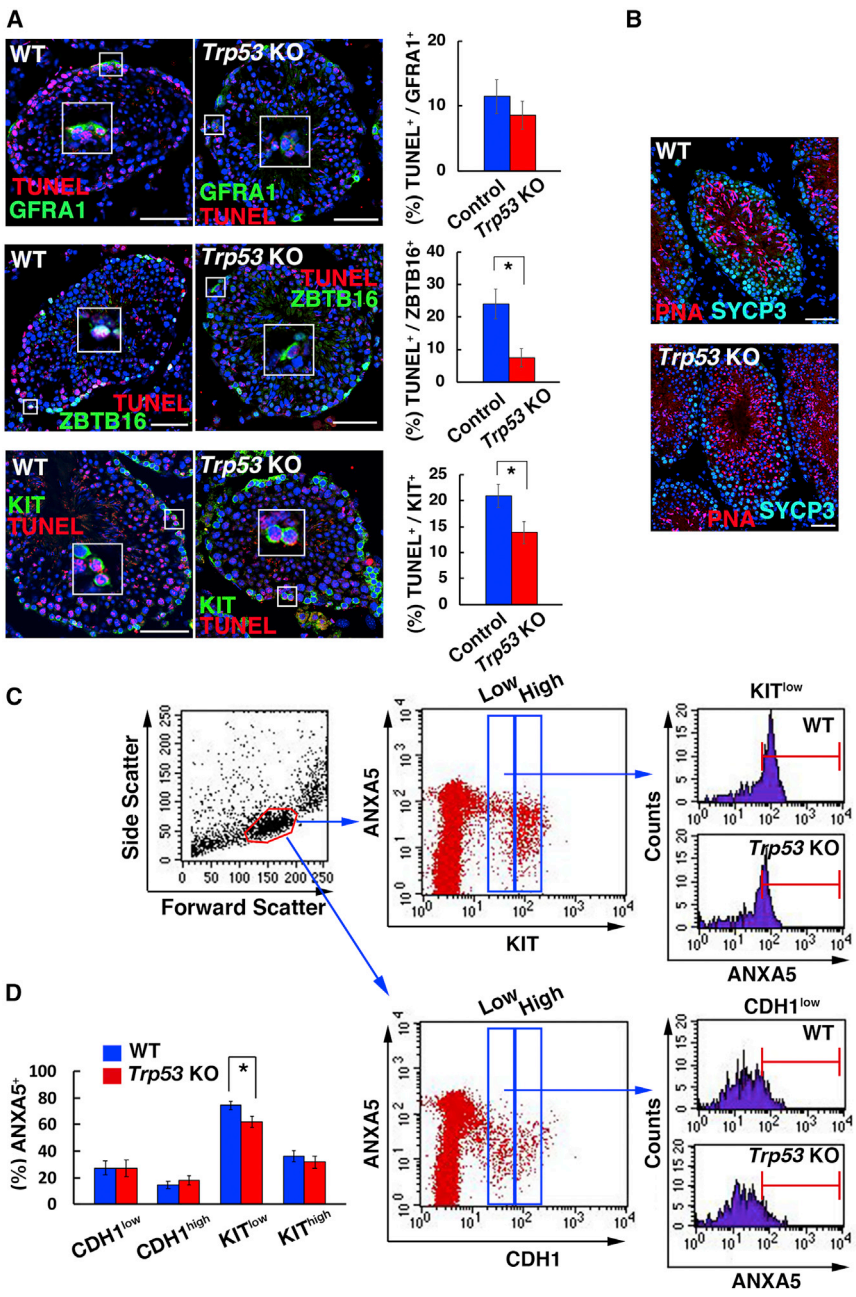

Figure 3. Reduced apoptosis of differentiating germ cells in *Trp53* KO mice

(A) TUNEL staining of *Trp53* KO testis with spermatogonium markers (n = 62 for GFRA1, n = 36 for ZBTB16, n = 66 for KIT).

(B) Immunostaining and lectin staining of spermatocyte (SCP3) and haploid cell (PNA) markers in *Trp53* KO testis.

(C) Flow cytometric analysis of apoptotic cells in *Trp53* KO testis. Cells were stained with ANXA5 and the indicated spermatogonium markers.

(D) Quantification of cell number (n = 8). Scale bars, 50 mm (A and B). Counterstain, Hoechst 33342 (A and B). Asterisks indicate statistical significance (*$p < 0.05$). See also Figure S4 and Table S2. Results are means ± SEM.

(Figure 3B). This result is consistent with a previous study (Huckins, 1978), which showed that only 25% of spermatogonia can survive during spermatogenesis. Similar results were obtained by CASP3 immunostaining (Figure S4A).

To confirm this observation, we performed flow cytometry analyses (Figure 3C). We first established a spermatogonium gate based on forward and side scatter values. We have shown previously that this gate contains SSCs and progenitor spermatogonia (Kanatsu-Shinohara et al., 2012). Although we did not find a significant difference in the number of apoptotic CDH1$^+$ undifferentiated spermatogonia, we noted that an increased number of KIT$^+$ differentiating germ cells reacted with the Annexin V stain (Figure 3D). These results suggested that lack of *Trp53* suppresses apoptosis of differentiating germ cells.

Transgenic offspring production using SSCs

We proposed that induction of clonal apoptosis of spermatogonia causes "clustering" of offspring with the same

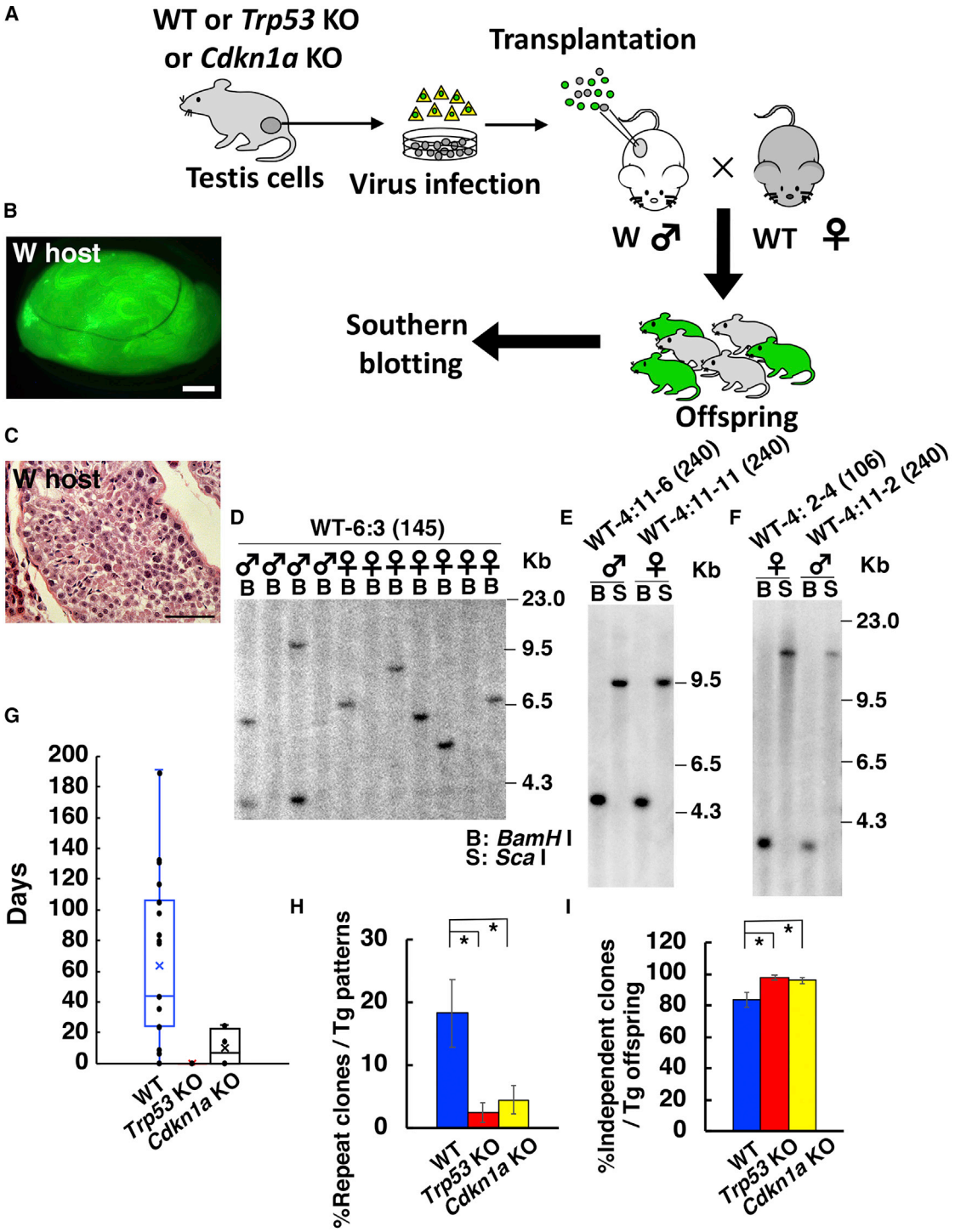

Figure 4. Transgenesis of SSCs and analysis of transgenic progeny

(A) Experimental schematic.

(B and C) Macroscopic (B) and histological (C) appearance of a recipient testis, showing spermatogenesis.

(D) Screening of transgenic offspring by Southern blot analysis using a *Venus* probe. The litter number is indicated above the gel (e.g., WT-6:3 indicates the third litter of recipient WT-6), and birth date after transplantation is shown in parentheses (145 days). *Bam*HI (B) does not cut the *Venus* probe. Therefore, each band after *Bam*HI digestion indicates integration of a single virus.

(legend continued on next page)

transgene integration patterns (Kanatsu-Shinohara et al., 2016). The reduced apoptosis and enhanced germline transmission of the *Trp53* KO allele implied that spermatogenesis from *Trp53* KO SSCs may produce offspring in a random pattern by producing a larger number of progenitor cells that would survive apoptosis. To test this hypothesis, we performed lentivirus-mediated gene delivery into SSCs for transgenerational lineage tracing (Figure 4A). Testis cells from *Trp53* KO and WT mice were collected and dissociated into single cells. These cells were exposed to the lentivirus CSII-EF-IRES-*Venus*, which contains the *Venus* gene under control of the *Eif1a* promoter. After overnight incubation, the cells were dissociated by trypsin digestion and microinjected into the seminiferous tubules of 8- to 10-day-old W mouse testes.

To confirm the transduction of SSCs, we sacrificed one of the recipients to confirm donor-derived spermatogenesis. Transplantation of lentivirus-infected testis cells produced numerous EGFP-expressing colonies 2 months after transplantation (Figure 4B). Histological analysis showed complete spermatogenesis from the transplanted SSCs (Figure 4C). Because this extensive colonization suggested restoration of fertility in recipient mice, the remaining recipient mice were housed with WT B6 females to produce offspring. The rate of offspring production, the size of the litter, and the number of litters were comparable regardless of donor cell type (Table S1).

To assess the transgene integration pattern into the genome, we performed Southern blot analysis using tail DNA from all offspring (Figure 4D). Each DNA was digested with restriction enzymes and hybridized with a *Venus*-specific probe. The identities of clones were confirmed using at least two different restriction enzymes (Figures 4E and 4F). When we identified multiple integrations, we followed each clone by using a different set of restriction enzymes. Analysis of W recipients with WT donor cells revealed that 106 of 381 offspring (27.8%) contained the *Venus* transgene, which suggested that 55.6% of SSCs were transduced because only one set of chromosomes would be transmitted to the offspring via meiosis. In contrast, a similar analysis of W mice with *Trp53* KO donor cells revealed that 101 of 289 offspring (34.9%) contained the *Venus* transgene. Although the value was higher for *Trp53* KO donor cells, there was no significant difference in transgenic offspring production efficiency. All offspring had a normal appearance without evidence of tumor formation. These results show that donor cell genotype does not significantly influence reproductive performance or transgenesis efficiency after spermatogonial transplantation (Figures S5A–S5C).

Clonal analysis of SSC contribution to offspring production

Based on the transgene integration patterns, we estimated the clonal variation of SSCs that sired the transgenic offspring. Consistent with our previous results (Kanatsu-Shinohara et al., 2016), offspring with the same virus integration patterns were found in different litters. We identified a mean of 12.4 different integration patterns from W mice that had received WT donor cells (Figure 5A). Six of the seven recipients produced offspring with the same transgene integration patterns (repeat clones). These repeats were found throughout the lifespan of the recipient mice. The recipient that did not sire repeat clones probably had poor fertility because it sired only 17 mice and produced only 3 transgenic mice. Although 71 clones appeared only once, 16 clones appeared at least twice; one of the clones appeared four times. Two clones appeared in the same litter (coincident clone). The mean lifespan of the clone, which was defined as the days between the first and the last appearance of the clone, was 63.9 days. The maximum lifespan was 191 days (Figure 4G). Because transfected progenitor cells would be lost after one cycle of spermatogenesis (35 days) because of lack of self-renewal activity, this result provides genetic evidence that single SSC clones undergo self-renewal division and produce offspring over a long-term period.

From the number of clonal types that appeared in the offspring from each recipient, we calculated the effective number of clones that actively participated in offspring production (active clones) based on maximum-likelihood estimations using data regarding the number of transplantable SSCs (504.4 per testis) (Kanatsu-Shinohara et al., 2016). Except for the one mouse that sired only three litters (WT-7), the estimated number of active clones was smaller in mice with repeat clones (Table S1). These results

(E and F) Confirmation of the clones in the same (E) or different (F) litters by Southern blot analysis using the *Venus* probe. Transgenic DNA identified in the initial screening was digested with *Bam*HI (B) or *Sca*I (S), which also does not cut the *Venus* probe. The same clone appeared in the 11th litter (clonal coincidence; 240 days after transplantation) (E), and another clone appeared in the second (106 days after transplantation) and 11th (240 days after transplantation) litters of the same recipient, WT-4 (F).

(G) Lifespan of SSC clones (n = 19 for WT, n = 2 for *Trp53* KO, n = 4 for *Cdkn1a*).

(H) Proportion of independent clones in all transgenic offspring (n = 5–7).

(I) Proportion of independent clones among transgenic offspring (n = 5–7).

Scale bar, 1 mm (B) and 50 μm (C). Counterstain, hematoxylin and eosin (C). Asterisks indicate statistical significance (*$p < 0.05$). See also Table S1. Results are means ± SEM.

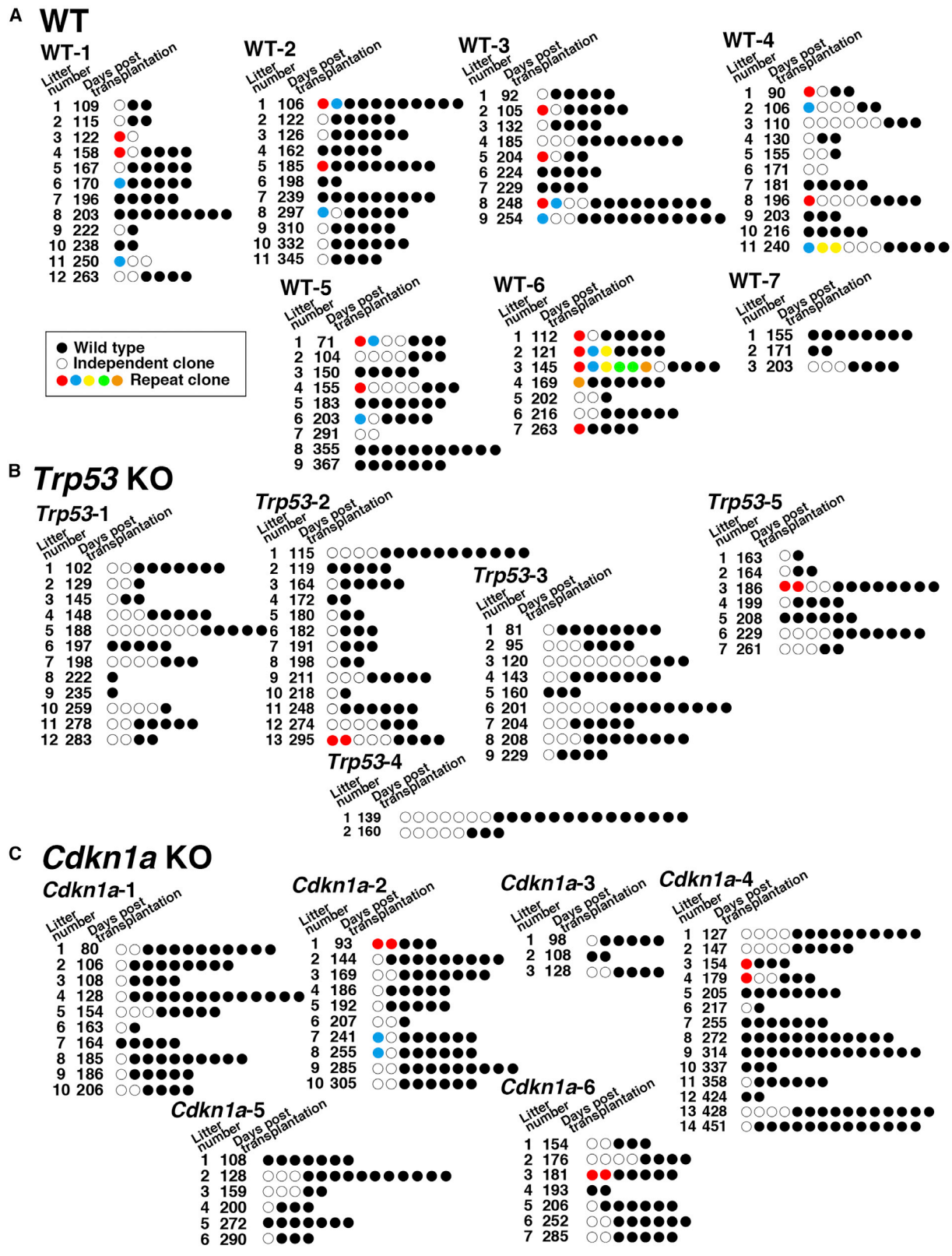

(legend on next page)

suggested that only a portion of SSCs contributes to offspring at a specific time point.

Analyses of transgenic offspring from *Trp53* KO donor cells showed a strikingly different germline transmission pattern (Figure 5B). Among 101 transgenic offspring, only 2 clones were identical. The proportion of repeat clones from *Trp53* KO cells (2.0%, 2 of 99 patterns) was significantly smaller than the proportion from WT cells (18.4%, 16 of 87 patterns). Consequently, we observed a larger number of clones from *Trp53* KO SSCs that exhibited different integrations patterns (Figure 4H). In each litter, 2.3 transgene integration patterns were found in offspring from *Trp53* KO SSCs, whereas 1.4 transgene integration patterns were found in offspring from WT SSCs. Because only two repeat clones appeared in 101 transgenic offspring from two recipients of *Trp53* KO SSCs, each transgenic offspring exhibited 0.98 (99 of 101) transgene integration patterns. In contrast, because 16 repeat clones appeared in 106 transgenic offspring, each transgenic offspring exhibited 0.82 (84 of 106) different integration patterns in WT SSCs. Therefore, *Trp53* KO donor cells produced offspring with greater genetic diversity (Figure 4I).

In terms of lifespan, because two clones with identical integration patterns were born in the same litter, all clones appeared only once during the lifetime (Figure 4G). Recipients continued to sire progeny for at least 295 days. Maximum-likelihood estimations indicated that the number of active SSCs in *Trp53* KO donor cells was significantly increased compared with those in WT donors (Table S1). Therefore, *Trp53* KO SSCs have a shorter lifespan and yield offspring with greater genetic diversity compared with WT SSCs.

Mathematical analysis of offspring production patterns

Using these data, the likelihood of producing offspring with the same transgene integration patterns was evaluated (Figure 6A). We hypothesized that each clone was randomly selected from a pool of SSC clones; we then calculated the frequency of clonal coincidence. We performed random sampling and evaluated the possibilities of obtaining the same clone in the same litter. When these values were compared with the actual number of litters that contained offspring with the same transgene integration patterns, the number of clone types in litters from the six WT SSCs was significantly smaller than the number expected based on random sampling calculations. Although we did not find statistical significance concerning offspring from the recipient (WT-7), this was likely due to the smaller number of offspring produced by this recipient (three litters) and the smaller number of transgenic clones (three clones). The remaining recipient mice produced 7–12 litters with more diverse patterns (8–25 clones). When the same analysis was performed involving offspring from *Trp53* KO donor SSCs, none of the five recipients showed statistical significance (Figure 6A). These results suggested that *Trp53* KO SSCs produced offspring in a random pattern.

To further investigate the dynamics of SSC offspring production patterns, we next analyzed repeat clones. We measured the minimum interval between births of offspring from the same clones. In our previous study, we analytically derived a probability distribution concerning the interval between births of the same clones (Kanatsu-Shinohara et al., 2016). When deriving this model, we assumed that each SSC clone spontaneously exhibited transient bursts of spermatogenic activity; we also reasoned that each burst was followed by a refractory period (Figure 6B). Based on these assumptions, we estimated that the cycle of each SSC burst was approximately 77.1 days.

Consistent with previous findings, repeat interval analysis of WT donor cells showed that offspring bearing the same integration patterns were not evenly distributed (Figure 6C). The frequency of the coincident clones in this study (3.2%, 2 of 62 litters) was slightly lower than the frequency in our previous study, which used a larger number of recipients (8.2%, 17 of 208 litters) (Kanatsu-Shinohara et al., 2016); however, seven clones appeared in the same or next litter in the current study (clonal burst). In contrast to our previous results, additional bursts were also found with longer intervals. When the observed results of the WT SSCs were compared with the model derived from the probability distribution of the inter-event intervals, no significant difference was found (Figure S6A), indicating that offspring production patterns from WT SSCs in this study follow the same kinetics that were observed in the early work. In contrast, the difference between *Trp53* KO SSCs and the model was striking. Although the relative frequency of coincident clones was higher (4.7%, 2 of 43 litters), there was no additional burst. Comparison of these results with the model showed a significant statistical difference (Figure S6B). These results suggested that offspring

Figure 5. Summary diagram of transgenic integration patterns

(A–C) All offspring from recipients that received (A) WT, (B) *Trp53* KO, or (C) *Cdkn1a* KO testis cell transplantation are indicated by the litter number and birth date after transplantation. Each circle represents offspring born after the indicated time points; black circles indicate offspring without transgenes. Clones with the identical colors from the same recipients are repeat clones. Offspring born on the same date were recorded as the same litter. The average numbers of virus integration in offspring were 1.9, 1.9, and 1.3 in WT, *Trp53* KO, and *Cdkn1a* KO SSCs, respectively. See also Figures S5 and S6.

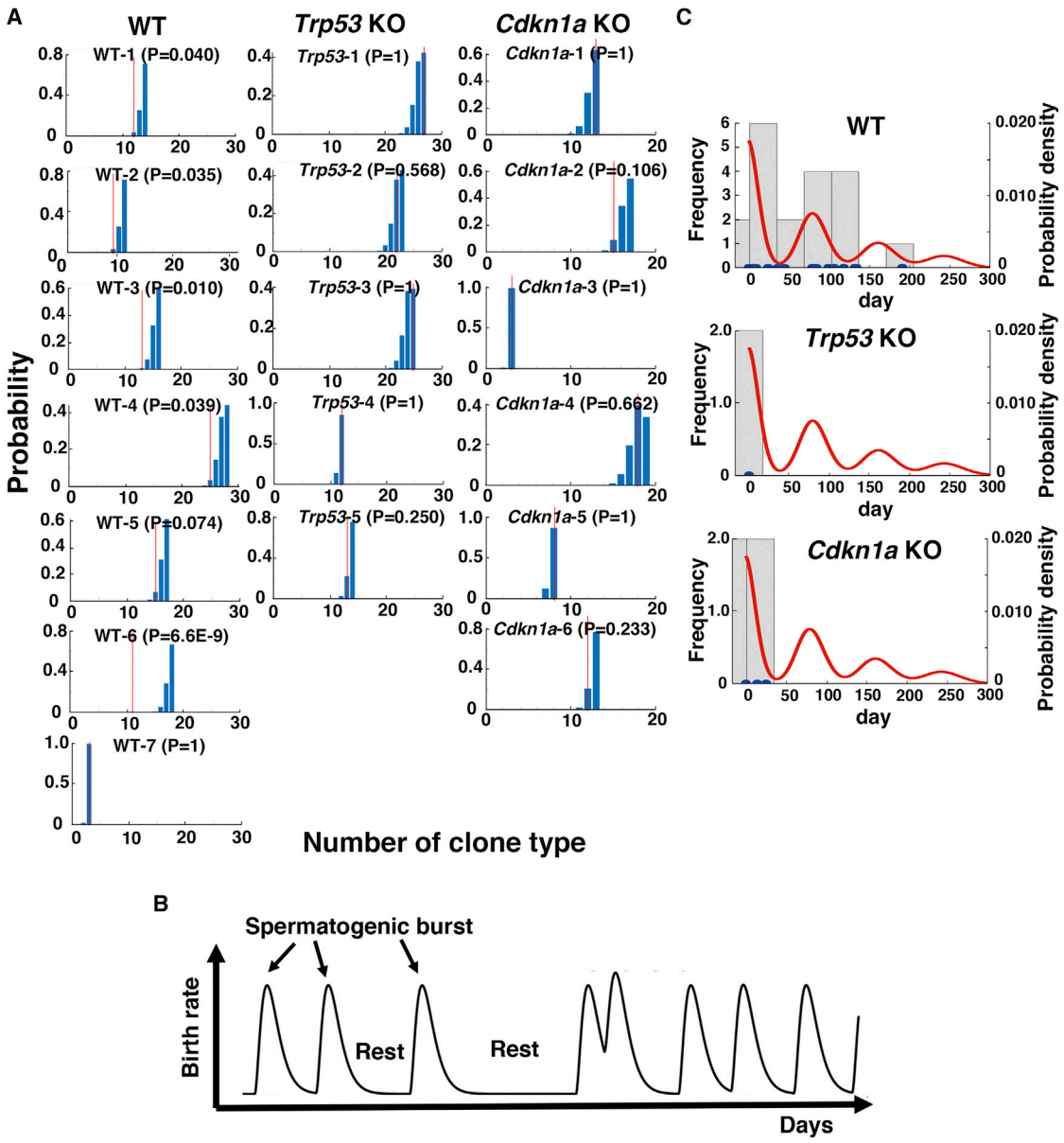

Figure 6. Integration pattern analysis

(A) Statistical testing for clonal variety among offspring derived from the same recipient. Blue columns indicate probability distribution of number of clone types, which was calculated by Monte Carlo sampling under the null hypothesis that each transfected progeny was randomly selected from a pool of active SSC clones (504.4 per testis; Kanatsu-Shinohara et al., 2016). Red bars indicate the actual number of clone types among offspring derived from the same recipient.

(B) Hypothetical model used to describe the spermatogenic activity of an SSC clone. SSCs are assumed to undergo spontaneous spermatogenic burst and rest cycles.

(C) Experimental data showing the minimum interval between birth of offspring with identical transgene integration patterns. The x axis represents the time after transplantation; the y axis indicates the actual number of offspring born within bin sizes of 34 days. Gray columns indicate the number of offspring born during the indicated period. Blue dots indicate the exact timing of birth. Red line indicates the probability distribution function based on historical samples (1,325 mice) using a model incorporating spermatogenic burst and rest (Kanatsu-Shinohara et al., 2016).

See also Figure S6.

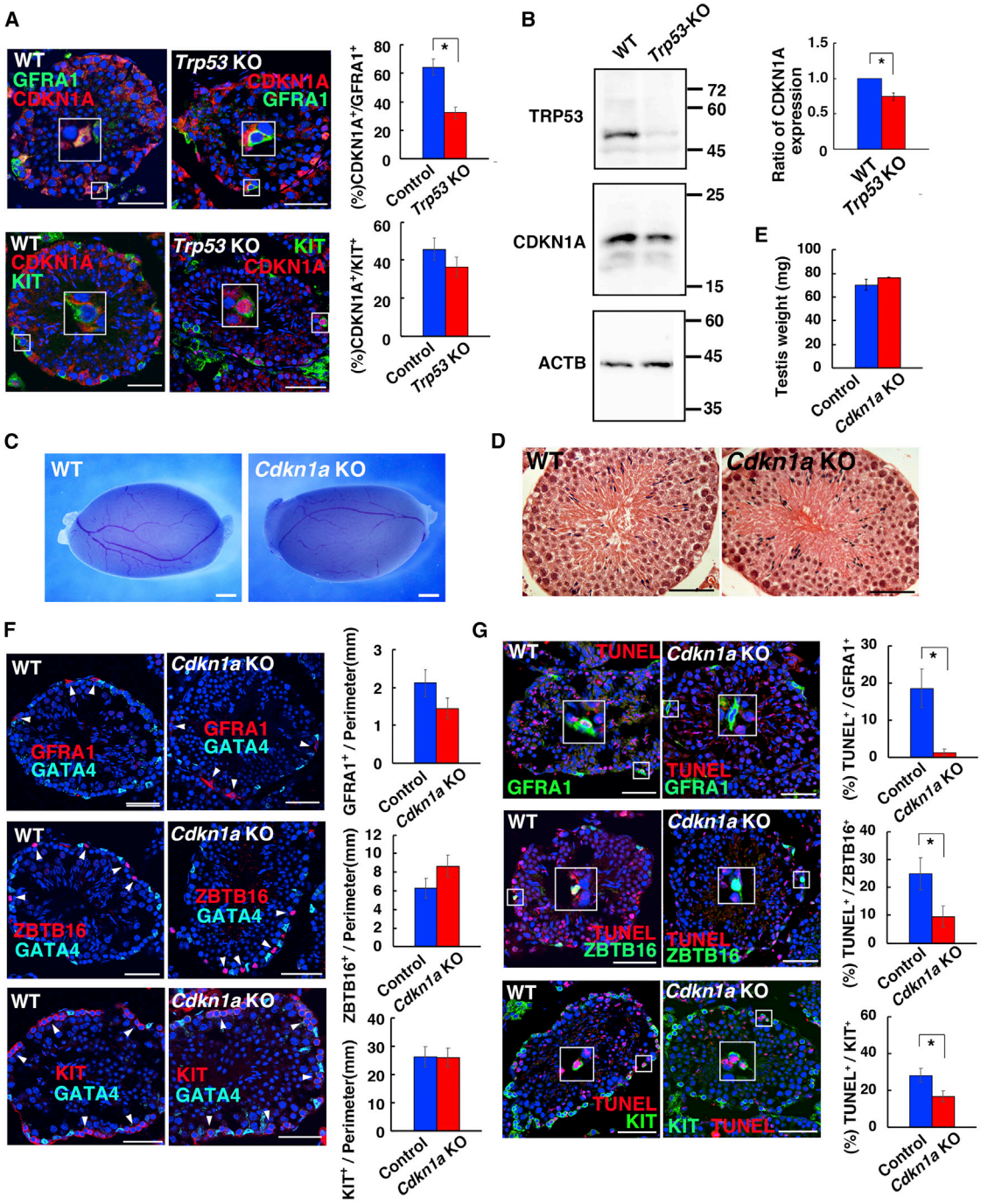

Figure 7. Reduced apoptosis of differentiating germ cells in *Cdkn1a* KO mice

(A) Double immunostaining of CDKN1A and spermatogonium markers in *Trp53* KO testis (n = 72–74 for GFRA1, n = 42–45 for KIT).

(B) Western blot analysis of CDKN1A in *Trp53* KO GS cells (n = 4).

(C) Macroscopic appearance of *Cdkn1a* KO testis.

(D) Histological appearance of *Cdkn1a* KO testis.

(E) Testis weight (n = 4).

(legend continued on next page)

production patterns from *Trp53* KO SSCs do not follow burst-rest cycles.

Suppression of apoptosis in Cdkn1a KO spermatogonia

The results in the preceding section showed that loss of *Trp53* increases the genetic diversity of the transgenic offspring. KO mouse models of various downstream targets of *Trp53* (*Bax*, *Apaf1*, and *Cdkn1a*) show spermatogenic abnormalities. However, *Bax* KO mice accumulate spermatogonia that cannot differentiate into sperm (Knudson et al., 1995). *Apaf1* KO mice show degeneration of spermatogenesis (Honarpour et al., 2000). Therefore, sperm formation efficiency is significantly reduced in these mutants, precluding analysis of their contributions to germline transmission patterns. In contrast, *Cdkn1a* KO mice reportedly exhibit macroorchidism with increased sperm production efficiency (Holsberger et al., 2005). Loss of *Cdkn1a* in Sertoli cells is considered to be responsible for this phenotype because of increased Sertoli cell numbers (Holsberger et al., 2005). However, more recent studies suggest that *Cdkn1a* KO spermatogenic cells have intrinsic abnormalities (Takubo et al., 2008; Morimoto et al., 2021). Therefore, we hypothesized that CDKN1A acts downstream of TRP53 in spermatogonia for predominant germline transmission.

We first directly compared the expression of CDKN1A in *Trp53* KO testes by immunostaining. The specificity of the anti-CDKN1A antibody was confirmed by immunostaining of *Cdkn1a* KO testes (Figure S1C). When the staining patterns were compared between KO and WT mice, a significant reduction of CDKN1A expression was found in GFRA1$^+$ undifferentiated *Trp53* KO spermatogonia compared with WT cells (Figure 7A). CDKN1A expression was also reduced in KIT$^+$ differentiating germ cells, although the degree of this reduction was smaller. We also noted dynamic changes in the localization of CDKN1A. In WT spermatogonia, 13.3% of GFRA1$^+$ spermatogonia (n = 15) and 26.7% of KIT$^+$ spermatogonia (n = 10) contained CDKN1A in the nucleus. On the other hand, 10.1% of GFRA1$^+$ spermatogonia (n = 13) and 18.0% of KIT$^+$ spermatogonia (n = 10) contained CDKN1A in *Trp53* KO spermatogonia. However, no statistical difference was found between KO and WT mice. Because these results suggested that TRP53 influences CDKN1A localization, we examined whether TRP53 is essential for CDKN1A induction. We used germline stem (GS) cell cultures to quantify CDKN1A expression (Kanatsu-Shinohara et al., 2003) because it is possible to collect a large number of SSCs from these cultures (Kanatsu-Shinohara and Shinohara, 2013). Western blot analysis of *Trp53* KO GS cells showed significant downregulation of CDKN1A (Figure 7B). These results suggest that the TRP53 regulates CDKN1A localization and its induction in spermatogonia.

To investigate the effect of *Cdkn1a* deficiency, we analyzed *Cdkn1a* KO mice. *Cdkn1a* KO testes do not show apparent changes in appearance (Figure 7C), and histological analysis revealed apparently normal spermatogenesis (Figure 7D). Consistent with previous reports, *Cdkn1a* KO testes were slightly larger than WT control testes (Figure 7E). Immunostaining revealed that the numbers of GFRA1$^+$ undifferentiated spermatogonia are comparable between *Cdkn1a* KO and WT testes (Figure 7F). Although there was no significant difference when we measured the numbers of ZBTB16$^+$ spermatogonia by tubule perimeter, a statistically significant increase in the number of ZBTB16$^+$ spermatogonia was found when the numbers of ZBTB16$^+$ cells per GATA4$^+$ Sertoli cells were compared (0.4 ± 0.1 versus 0.7 ± 0.1 per GATA4$^+$ cells; n = 30–35). Therefore, we presumed that *Cdkn1a* deficiency might have caused abnormalities in committed spermatogonium progenitor cells. Consistent with these observations, we noted enhanced mitotic activity in KIT$^+$ differentiating germ cells (Figure S3B). TUNEL staining showed significantly fewer apoptotic cells in all stages (Figure 7G). These results implied that *Cdkn1a* acts downstream of *Trp53* and influences germline transmission patterns through regulation of apoptosis in differentiating germ cells.

Transgenerational lineage analysis of Cdkn1a SSCs

To examine the germline transmission patterns of *Cdkn1a* KO SSCs, we collected pup testes, and the cells were transplanted into W recipients for transgenerational lineage analysis. Overall, the reproductive performance of the *Cdkn1a* KO recipient mice was comparable with the performance of WT and *Trp53* KO recipient mice (Table S1). Southern blot analysis of tail DNA showed that lentivirus transduction had successfully produced transgenic mice from six recipient mice. The proportion of transgenic offspring was 19.9%, which was lower than the proportions of transgenic offspring from WT (27.8%) or *Trp53* KO (34.9%) SSCs (Table S1). However, there were no significant differences among the groups. Southern blot analysis

(F) Double immunostaining for a Sertoli cell marker (GATA4) and spermatogonia markers in *Cdkn1a* KO testis (n = 38 for GFRA1, n = 33 for ZBTB16, n = 34 for KIT).

(G) TUNEL staining of *Cdkn1a* KO testis with spermatogonium markers (n = 33 for GFRA-1, n = 31–35 for ZBTB16, n = 40 for KIT).

Scale bars, 50 μm (A, D, F, and G) and 1 mm (C). Counterstain, Hoechst 33,342 (A, F, and G) and hematoxylin and eosin (D). Asterisks indicate statistical significance ($p < 0.05$). See also Figures S1, S3–S7, and Table S2. Results are means ± SEM.

revealed 69 different transgene integration patterns in a total of 73 transgenic offspring from *Cdkn1a* KO SSCs (Figure 5C). Of the six recipient mice, three were able to sire four repeat clones, which was significantly reduced compared with WT cells. Two of the clones were born in the same litter. The maximum lifespan was 25 days; the mean lifespan was 9.8 days. Therefore, the mean lifespan of the clones was significantly shorter than the mean lifespan of WT SSCs.

When the number of active clones was estimated by maximum likelihood estimations, the number tended to be smaller in recipients with these repeat clones, similar to the findings concerning *Trp53* KO donor cells. A mean of 1.5 transgenic mice was born per litter, which was comparable with the findings in WT and *Trp53* KO donor cells. However, because 4 repeat clones were found among 73 transgenic offspring from *Cdkn1a* KO SSCs, each transgenic offspring exhibited 0.95 (69 of 73) transgene integration patterns. Although this value was significantly higher than the value of WT donor cells (0.82 [84 of 106]), it was comparable with the value of *Trp53* KO donor cells (0.98 [99 of 101]). These results suggest that *Cdkn1a* deficiency increases the genetic diversity of offspring.

Based on these data, we performed a random sampling analysis to evaluate the likelihood of producing offspring with the same transgene integration pattern. Like *Trp53* KO SSCs, the numbers of clone types in litters from the six WT SSCs were comparable with the number expected from the random sampling analysis (Figure 6A). Repeat interval analysis showed that the frequency of coincident clones was comparable (4.0%) with the frequencies of WT (3.2%) or *Trp53* KO (4.7%) donor cells. However, because all repeat clones were found in the same or the next litter, there were no additional bursts with longer intervals (Figure 6C). Statistical comparison of the observed results for *Cdkn1a* KO SSCs and the model derived from the probability distribution of the inter-event intervals showed a significant difference (Figure S6C). These results suggest that *Cdkn1a* acts downstream of *Trp53* to inhibit genetic diversity in the offspring from SSCs by producing offspring in random patterns.

DISCUSSION

This study was undertaken to identify genes involved in male germline transmission pattern formation. Although many infertile mutants are available, identification of mutants with defective pattern formation is difficult because such mutants do not necessarily exhibit fertility defects. We presumed that fertile KO mice with abnormal histology may provide a clue to approach this problem. We focused on *Fmr1* because mice lacking *Fmr1* exhibit macroorchidism (Slegtenhorst-Eegdeman et al., 1998). *Trp53* was chosen because *Trp53* KO mice exhibit decreased apoptosis and production of spermatozoa with abnormal morphology (Beumer et al., 1998). In our initial experiments, we performed competitive transplantation assays to determine the possibility of abnormal germline transmission. Although *Fmr1* KO SSCs did not show an apparent phenotype, *Trp53* KO SSCs showed excessive production of offspring with the mutant allele despite abnormal spermatogenesis. Based on our hypothesis, we tested whether *Trp53* plays a role in germline transmission pattern formation.

Trp53 is a tumor suppressor gene (Levine et al., 2016). Because *Trp53* KO mice produced abnormal sperm and sired fewer offspring, it has been suggested that loss of *Trp53* is involved in germ cell quality control (Yin et al., 1998). Although the number of sperm in *Trp53* KO mice is comparable with that of WT mice (Zalzali et al., 2018), sperm motility is decreased (Schwartz et al., 1999). Therefore, it was reasonable to think that WT cells have competitive advantage over *Trp53* KO cells. However, *Trp53* KO SSCs outcompeted WT SSCs and produced more offspring by competitive spermatogonial transplantation. The most straightforward explanation for the superiority over WT SSCs was extensive self-renewal of *Trp53* KO SSCs because *Trp53* limits the self-renewal division of many tissue-specific stem cells (Bonizzi et al., 2012). For example, neural stem cells lacking *Trp53* showed increased survival and proliferation (Meletis et al., 2006). *Trp53* also negatively regulates hematopoietic stem cells and mammary stem cells (Cicalese et al., 2009; Liu et al., 2009). However, when this hypothesis was tested by serial spermatogonial transplantation, neither SSC number nor self-renewal activity showed abnormalities in *Trp53* KO mice. Therefore, enhanced germline transmission could not be explained by SSC activity. Because competitive transplantation experiments were performed in a WT environment and *Trp53* is also expressed in somatic cells, our results suggest that the poor reproductive performance of *Trp53* KO mice was indirectly caused by defects in somatic cells.

An alternative explanation for the enhanced germline transmission of *Trp53* KO SSCs is increased production of progenitor cells. Although we cannot totally exclude the possibility that *Trp53* deficiency conferred a selective advantages in meiotic or haploid germ cells, these cells lack mitotic activity and cannot dramatically increase their numbers. In contrast, a previous study showed a 40% increase in the total number of A spermatogonia (Beumer et al., 1998). Therefore, we initially expected an increased number of KIT^+ germ cells. Instead, the number of $CDH1^+$ or $SOX3^+$ undifferentiated spermatogonia was

increased without significant changes in KIT$^+$ spermatogonium number. However, the exact identity of cell types is difficult to determine by immunostaining because these genes (*Zbtb16*, *Kit*, *Cdh1*, and *Trp53*) influence each other (Filipponi et al., 2007; Oikawa et al., 2018; Gao et al., 2019). For example, although ZBTB16 and CDH1 have essentially identical expression patterns in WT mice (Nakagawa et al., 2010), only *Cdh1* is downregulated in *Trp53* KO mice (Liu et al., 2022), which suggested that these two genes are regulated differentially. Apoptosis was significantly reduced in ZBTB16$^+$ or KIT$^+$ spermatogonia. However, given that the number of SSCs was comparable between *Trp53* KO and WT mice and considering the increased number of CDH1$^+$ or SOX3$^+$ spermatogonia, these results suggest that the number of committed spermatogonia is increased in *Trp53* KO testes. Such an increase in progenitor fraction was suggestive of random offspring production because the clones of germ cells that would have been lost during normal spermatogenesis likely survive without *Trp53*; therefore, more diverse clones can contribute to fertilization (Kanatsu-Shinohara et al., 2016).

Consistent with our hypothesis, our analysis of integration patterns suggested that SSCs in the *Trp53* KO mice rarely produced transgenic offspring with the same transgene integration patterns. This appears to contradict the results of the serial transplantation experiments, which showed comparable behavior between *Trp53* KO and WT SSCs. We think that this discrepancy may be caused by the difference in testis microenvironment in which the assays were performed and the difference in detection methods. In the serial transplantation assay, because SSCs were microinjected into the empty seminiferous tubules, SSCs proliferated freely, and the interaction with other clones probably did not occur (Nagano et al., 1999). Therefore, we could observe all SSC clones. In contrast, the recipient testes are full of germ cells in the case of lineage analysis. In such testes, SSCs are competing with each other for fertilization. We can only detect the activity of SSCs by the presence of the transgene in the offspring. Therefore, we cannot identify the behavior of SSCs unless they make transgenic offspring.

The possibility that *Trp53* regulates differentiation patterns has largely been ignored because strong developmental defects have not been observed in KO mice (Jain and Barton, 2018). However, the lack of developmental defects does not necessarily mean that differentiation occurred in a physiological manner. To our knowledge, there has been no clonal analysis study of *Trp53* KO mice, and the effect of *Trp53* on differentiation patterns has not been evaluated. However, our study suggests that *Trp53* deficiency can increase the number of clones that would have been lost during differentiation. Such abnormalities may be obscured during tissue turnover, in which somatic cells gradually disappear and are lost; however, increased clone numbers could influence the outcome of a bottleneck selection process such as fertilization. Because loss of *Trp53* does not compromise fertility, this could be overlooked. Thus, the discrepancy between the serial transplantation experiments and lineage analysis suggested that *Trp53* limits germline genetic diversity by restricting the number of SSC clones for fertilization.

Among the numerous *Trp53* target genes, we found that *Cdkn1a* is responsible for an abnormal germline transmission pattern. *Cdkn1a* was discovered as a transcriptionally activated target of *Trp53* (El-Deiry et al., 1993). Although the effect of *Cdkn1a* on testis abnormalities are considered to be mediated by Sertoli cells (Holsberger et al., 2005), we sought abnormalities in spermatogonia and noted a significant reduction in apoptotic cells. Consistent with the reduced apoptosis in *Cdkn1a* KO mice, *Cdkn1a* KO SSCs also showed abnormal germline transmission patterns in a manner similar to *Trp53* KO SSCs. More extensive suppression of spermatogonium apoptosis in *Cdkn1a* KO mice was unexpected because *Cdkn1a* KO mice exhibit a minor phenotype compared with *Trp53* KO mice. Downregulation of CDKN1A expression in *Trp53* KO GS cells *in vitro* and undifferentiated spermatogonia *in vivo* suggested that CDKN1A acts downstream of TRP53. Therefore, our results indicate that the TRP53-CDKN1A pathway restricts the diversification of male germline cells (Figure S7).

Although the biological significance of clonal spermatogonial apoptosis has long remained unknown, our results provide insight into the role of apoptosis in germline transmission patterns. *Trp53* has been presumed to play a role in protecting genome stability in the germline (Levine et al., 2016); however, our study suggests that *Trp53*-mediated apoptosis has a role in regulating the genetic diversity of the male germline. Abnormalities in clonal apoptosis may be manifested as a lack of periodicity in SSC-derived offspring. Such an abnormal germline transmission pattern may contribute to the paternal age effect, in which some spontaneous disorders tend to arise more frequently in the progeny of older men (Maher et al., 2014). Because regulation of *Trp53* expression differs between mice and humans (Jaworski et al., 2005), the involvement of the *Trp53*-*Cdkn1a* pathway in human paternal age effect is unknown; however, the RAS pathway, which is often involved in human paternal age effects (Maher et al., 2014), regulates *Trp53* (Ries et al., 2000). TRP53 also controls RAS in humans (Jaworski et al., 2005). The next important goal is to understand how specific clones are selected for germline transmission. Our identification of genes involved in germline transmission patterns provides insights into

the molecular mechanism of genetic variation, disease, and evolution.

EXPERIMENTAL PROCEDURES

Animals and transplantation

Trp53 KO mice were provided by RIKEN BRC (B6.Cg-Trp53,tm1Sia>/Rbrc; stock number RBRC01361; Tsukuba, Japan). *Fmr1* KO mice (B6.129P2-Fmr1^{tm1Cgr}/J; stock number 003025) and *Cdkn1a* KO mice (B6; 129S2-Cdkn1a^{tm1Tyj}/J; stock number 003263) were purchased from Jackson Laboratory (Bar Harbor, ME). C57BL/6 Tg14(act-EGFP)OsbY01(Green) mice were a gift from Dr. M. Okabe (Osaka University, Osaka, Japan). W mice were purchased from Japan SLC (Shizuoka, Japan). We also used CB-17 severe combined immunodeficiency (SCID) mice for immunostaining of TRP53 and FMR1 (Japan CLEA, Tokyo, Japan). Testis cells were dissociated into single cells by a two-step enzymatic digestion protocol using type IV collagenase and trypsin (Ogawa et al., 1997). For production of offspring, immature testes were collected from 5- to 10-day-old mice. Donor cells were suspended at 3×10^7 cells/mL and transplanted into the seminiferous tubules of 5- to 10-day-old W mice. For serial transplantation, donor cells were suspended at 1×10^8 cells/mL and transplanted into 4- to 5-week-old W mice. All injections were performed through the efferent duct. Approximately 2 or 10 μL of cell suspension was microinjected into pups or mature testes, respectively. Each injection filled 80%–90% of the seminiferous tubules. The Institutional Animal Care and Use Committee of Kyoto University approved all animal experimental protocols.

Probability distribution of the inter-birth interval for the same clone

We previously modeled the spermatogenic activity of SSC clones as a stochastic process in combination with an inhomogeneous Poisson process and Gamma process, as follows. Births of clonal progeny are selected by an inhomogeneous Poisson process with a time-dependent rate $r(t)$:

$$r(t) = \sum_i f(t - \xi_i),$$

where $f(t)$ is a transiently increased function during spermatogenic burst activity, and ξ_i indicates a timing of the ith initiation of the spermatogenic burst. Thus, $r(t)$ is determined by a summation of multiple transient bursts of spermatogenic activity. We employed the following transiently increasing function $f(t)$:

$$(t) = \alpha \frac{t^{k_f - 1}\exp(-t/\theta_f)}{\Gamma(k_f)\theta_f^{k_f}} H(t),$$

where α indicates a parameter regulating the amplitude, and k_f and θ_f indicate the shape and scale parameters, respectively. $\Gamma(x)$ is a Gamma function of x, and $H(t)$ is a Heaviside step function. If spermatogenic bursts are not accompanied by refractory periods, then these timings do not simply obey a Poisson process; instead, they obey a Gamma process, in which inter-burst intervals (e.g., $\Xi_i = \xi_i - \xi_{i-1}$), are sampled from a Gamma distribution:

$$G(\Xi_i|k_p, \theta_p) = \frac{\Xi_i^{k_p - 1}\exp(-\Xi_i/\theta_p)}{\Gamma(k_p)\theta_p^{k_p}},$$

where k_p and θ_p indicate the shape parameter and scale parameters, respectively. Previously, we derived a probability distribution of inter-birth intervals (Kanatsu-Shinohara et al., 2016):

$$P(\tau) = \int_0^\infty \bar{r}(\tau + u)\exp\left(-\int_0^\tau \bar{r}(s + u)ds\right)P'(u)du,$$

where

$$\bar{r}(t) = f(t) + \sum_i \int_0^\infty f(t - s)G(s|ik_p, \theta_p)ds,$$

and

$$P'(t) = \frac{f(t)\exp(-\int_0^s f(s)ds)}{\int_0^\infty f(x)\exp(-\int_0^x f(s)ds)dx}.$$

Parameters were estimated only from previous data (Kanatsu-Shinohara et al., 2016), as $\alpha = 0.612$, $k_f = 26.165$, $\theta_f = 1.911$, $k_f = 57.208$, and $\theta_p = 1.447$.

Evaluation of clonal coincidence

To evaluate the repetition of the clonal types from offspring, we mathematically described the clonal selection process. We modeled it as the following stochastic process: there are N different colored balls in a box, and we independently and randomly select a ball from the box m times and return it. N and m correspond to the number of clones in the testis and the number of observed offspring, respectively. Here we calculated $P(x, m)$, the probability that x clonal types are observed until the mth offspring, as recurrence formula:

$$P(x, m + 1) = P(x, m) - \frac{N - x}{N}P(x, m) + \frac{N - (x - 1)}{N}P(x - 1, m).$$

The second and third terms describe the probability that a new clone is selected at the m+1th offspring and the probability that an already selected clone is selected at the m+1th offspring, respectively. Based on the recurrence equation, the probability distribution of x given m and N can be calculated. This probability distribution was used for statistical testing to test whether clonal coincidence occurred significantly. Because all clones were unlabeled, we replaced N with $[2sN]$ in the statistical testing, where s denotes the ratio of transgenic offspring, and [] indicates a rounding function.

Statistical analyses

Significant differences between means for single comparisons were determined by Student's t test. The Kolmogorov-Smirnov test was used to evaluate the significance of differences between analytically derived probability density function and real data.

SUPPLEMENTAL INFORMATION

Supplemental information can be found online at https://doi.org/10.1016/j.stemcr.2022.07.007.

AUTHOR CONTRIBUTIONS

T.S. and M.K.-S. conceived the idea and designed the study. T.S., T.T., and M.K.-S. performed the experiments, M.T., T.K., and N.O. contributed a new reagent, and T.S., H.N., T.Y. and M.K.-S. analyzed data. T.S., H.N. and M.K.-S. wrote the manuscript.

ACKNOWLEDGMENTS

We thank Dr. Kana Yoshido for statistical analysis. Financial support for this research was provided by The Uehara Memorial Foundation, AMED (17933225 and JP21gm1110008), and MEXT (19K22512, 19H05750, 19H04906, 18H04882, 18H05281, and 18H02935).

CONFLICTS OF INTEREST

The authors declare no competing interests.

Received: January 19, 2022
Revised: July 10, 2022
Accepted: July 10, 2022
Published: August 4, 2022

REFERENCES

Bakker, C.E., Verheij, C., Willemsen, R., van der Helm, R., Oerlemans, F., Vermey, M., Bygrave, A., Hoogeveen, A.T., Oostra, B.A., Reyniers, E., et al. (1994). Fmr1 knockout mice: a model to study fragile X mental retardation. Cell *78*, 23–33.

Bächner, D., Stéinbach, P., Wöhrle, D., Just, W., Vogel, W., Hameister, H., Manca, A., and Poustka, A. (1993). Enhanced Fmr1 expression in testis. Nat. Genet. *4*, 115–116.

Beumer, T.L., Roepers-Gajadien, H.L., Gademan, I.S., van Buul, P.P., Gil-Gomez, G., Rutgers, D.H., and de Rooij, D.G. (1998). The role of the tumor suppressor p53 in spermatogenesis. Cell Death Differ. *5*, 669–677.

Bonizzi, G., Cicalese, A., Insinga, A., and Pelicci, P.G. (2012). The emerging role of p53 in stem cells. Trends Mol. Med. *18*, 6–12.

Boyer, A., Zhang, X., Levasseur, A., Abou Nader, N., St-Jean, G., Nagano, M.C., and Boerboom, D. (2021). Constitutive activation of CTNNB1 results in a loss of spermatogonial stem cell activity in mice. PLoS One *16*, e0251911.

Buageaw, A., Sukhwani, M., Ben-Yehudah, A., Ehmcke, J., Rawe, V.Y., Pholpramool, C., Orwig, K.E., and Schlatt, S. (2005). GDNF faily receptor alpha1 phenotype of spermatogonial stem cells in immature mouse testes. Biol. Reprod. *73*, 1011–1016.

Cicalese, A., Bonizzi, G., Pasi, C.E., Faretta, M., Ronzoni, S., Giulini, B., Brisken, C., Minucci, S., Di Fiore, P.P., and Pelicci, P.G. (2009). The tumor suppressor p53 regulates polarity of self-renewing divisions in mammary stem cells. Cell *138*, 1083–1095.

de Rooij, D.G. (2017). The nature and dynamics of spermatogonial stem cells. Development *144*, 3022–3030.

Devys, D., Lutz, Y., Rouyer, N., Bellocq, J.-P., and Mandel, J.-L. (1993). The FMR-1 protein is cytoplasmic, most abundant in neurons and appears normal in carriers of a fragile X premutation. Nat. Genet. *4*, 335–340.

Ebata, K.T., Zhang, X., and Nagano, M.C. (2005). Expression patterns of cell-surface molecules on male germ line stem cells during postnatal mouse development. Mol. Reprod. Dev. *72*, 171–181.

El-Deiry, W.S., Tokino, T., Velculescu, V.E., Levy, D.B., Parsons, R., Trent, J.M., Lin, D., Mercer, W.E., Kinzler, K.W., and Vogelstein, B. (1993). WAF1, a potential mediator of p53 tumor suppression. Cell *75*, 817–825.

Filipponi, D., Hobbs, R.M., Ottolenghi, S., Rossi, P., Jannini, E.A., Pandolfi, P.P., and Dolci, S. (2007). Repression of kit expression by Plzf in germ cells. Mol. Cell Biol. *27*, 6770–6781.

Fleischman, R.A. (1993). From white spots to stem cells: the role of the Kit receptor in mammalian development. Trends Genet. *9*, 285–290.

Gao, X., Chen, H., Liu, J., Shen, S., Wang, Q., Clement, T.M., Deskin, B.J., Chen, C., Zhao, D., Wang, L., et al. (2019). The REGγ-proteasome regulates spermatogenesis partially by P53-PLZF signaling. Stem Cell Rep. *13*, 559–571.

Hamer, G., Roepers-Gajadien, H.L., Gademan, I.S., Kal, H.B., and de Rooij, D.G. (2003). Intercellular bridges and apoptosis in clones of male germ cells. Int. J. Androl. *26*, 348–353.

Hara, K., Nakagawa, T., Enomoto, H., Suzuki, M., Yamamoto, M., Simons, B.D., and Yoshida, S. (2014). Mouse spermatogenic stem cells continuously interconvert between equipotent singly isolated and syncytial states. Cell Stem Cell *14*, 658–672.

Harper, M.J.K. (1982). Sperm and egg transport. In Germ Cells and Fertilization, C.R. Austin and R.V. Short, eds. (Cambridge University Press), pp. 102–127.

Honarpour, N., Du, C., Richardson, J.A., Hammer, R.E., Wang, X., and Herz, J. (2000). Adult Apaf-1-deficient mice exhibit male infertility. Dev. Biol. *218*, 248–258.

Holsberger, D.R., Buchold, G.M., Leal, M.C., Kiesewetter, S.E., O'Brien, D.A., Hess, R.A., França, L.R., Kiyokawa, H., and Cooke, P.S. (2005). Cell-cycle inhibitors $p27^{Kip1}$ and $p21^{Cip}$ regulate murine Sertoli cell proliferation. Biol. Reprod. *72*, 1429–1436.

Huckins, C. (1978). The morphology and kinetics of spermatogonial degeneration in normal adult rats: an analysis using a simplified classification of the germinal epithelium. Anat. Rec. *190*, 905–926.

Jain, A.K., and Barton, M.C. (2018). p53: emerging roles in stem cells, development and beyond. Development *145*, dev158360.

Jaworski, M., Hailfinger, S., Buchmann, A., Hergenhahn, M., Hollstein, M., Ittrich, C., and Schwarz, M. (2005). P53 knock-in (hupki) mice do not differ in tumor response from their counterparts with murine p53. Carcinogenesis *26*, 1829–1834.

Kanatsu-Shinohara, M., Ogonuki, N., Inoue, K., Miki, H., Ogura, A., Toyokuni, S., and Shinohara, T. (2003). Long-term proliferation in culture and germline transmission of mouse male germline stem cells. Biol. Reprod. *69*, 612–616.

Kanatsu-Shinohara, M., Inoue, K., Miki, H., Ogonuki, N., Takehashi, M., Morimoto, T., Ogura, A., and Shinohara, T. (2006). Clonal origin of germ cell colonies after spermatogonial transplanation in mice. Biol. Reprod. *75*, 68–74.

Kanatsu-Shinohara, M., Morimoto, H., and Shinohara, T. (2012). Enrichment of mouse spermatogonial stem cells by melanoma cell adhesion molecule expression. Biol. Reprod. *87*, 139–210.

Kanatsu-Shinohara, M., and Shinohara, T. (2013). Spermatogonial stem cell self-renewal and development. Annu. Rev. Cell Dev. Biol. *29*, 163–187.

Kanatsu-Shinohara, M., Naoki, H., and Shinohara, T. (2016). Nonrandom germline transmission of mouse spermatogonial stem cells. Dev. Cell *38*, 248–261.

Knudson, C.M., Tung, K.S., Tourtellotte, W.G., Brown, G.A., and Korsmeyer, S.J. (1995). Bax-deficient mice with lymphoid hyperplasia and male germ cell death. Science *270*, 96–99.

Levine, A.J., Puzio-Kuter, A.M., Chan, C.S., and Hainaut, P. (2016). The role of the p53 protein in stem-cell biology and epigenetic regulation. Cold Spring Harb. Perspect. Med. *6*, a026153.

Liu, S., Wei, R., Liu, H., Liu, R., Li, P., Zhang, X., Wei, W., Zhao, X., Li, X., Yang, Y., et al. (2022). Analysis of chromatin accessibility in p53 deficient spermatogonial stem cells for high frequency transformation into pluripotent state. Cell Prolif. *55*, e13195.

Liu, Y., Elf, S.E., Miyata, Y., Sashida, G., Liu, Y., Huang, G., Di Giandomenico, S., Lee, J.M., Deblasio, A., Menendez, S., et al. (2009). p53 regulates hematopoietic stem cell quiescence. Cell Stem Cell *4*, 37–48.

Maher, G.J., Goriely, A., and Wilkie, A.O.M. (2014). Cellular evidence for selfish spermatogonial selection in aged human testes. Andrology *2*, 304–314.

McAninch, D., Mäkelä, J.A., La, H.M., Hughes, J.N., Lovell-Badge, R., Hobbs, R.M., and Thomas, P.Q. (2020). SOX3 promotes generation of committed spermatogonia in postnatal mouse testes. Sci. Rep. *10*, 6751.

Meistrich, M.L., and van Beek, M.E.A.B. (1993). Spermatogonial stem cells. In Cell and Molecular Biology of the Testis, C.C. Desjardins and L.L. Ewing, eds. (Oxford University Press), pp. 266–295.

Meletis, K., Wirta, V., Hede, S.M., Nistér, M., Lundeberg, J., and Frisén, J. (2006). p53 suppresses the self-renewal of adult neural stem cells. Development *133*, 363–369.

Morimoto, H., Yamamoto, T., Miyazaki, T., Ogonuki, N., Ogura, A., Tanaka, T., Kanatsu-Shinohara, M., Yabe-Nishimura, C., Zhang, H., Pommier, Y., et al. (2021). An interplay of NOX1-derived ROS and oxygen determines the spermatogonial stem cell self-reewal efficiency under hypoxia. Genes Dev. *35*, 250–260.

Nagano, M., Avarbock, M.R., and Brinster, R.L. (1999). Pattern and kinetics of mouse donor spermatogonial stem cell colonization in recipient testes. Biol. Reprod. *60*, 1429–1436.

Nakagawa, T., Sharma, M., Nabeshima, Y.-I., Braun, R.E., and Yoshida, S. (2010). Functional hierarchy and reversibility within the murine spermatogenic stem cell compartment. Science *328*, 62–67.

Oatley, M.J., Racicot, K.E., and Oatley, J.M. (2011). Sertoli cells dictate spermatogonial stem cell niches in the mouse testis. Biol. Reprod. *84*, 639–645.

Ogawa, T., Aréchaga, J.M., Avarbock, M.R., and Brinster, R.L. (1997). Transplantation of testis germinal cells into mouse seminiferous tubules. Int. J. Dev. Biol. *41*, 111–122.

Oikawa, T., Otsuka, Y., Onodera, Y., Horikawa, M., Handa, H., Hashimoto, S., Suzuki, Y., and Sabe, H. (2018). Necessity of p53-binding to the CDH1 locus for its expression defines two epithelial cell types differing in their integrity. Sci. Rep. *8*, 1595.

Ries, S., Biederer, C., Woods, D., Shifman, O., Shirasawa, S., Sasazuki, T., McMahon, M., Oren, M., and McCormick, F. (2000). Opposing effects of Ras on p53: transcriptional activation of mdm2 and induction of $p19^{ARF}$. Cell *103*, 321–330.

Russell, L.D., Ettlin, R.A., Sinha Hikim, A.P., and Clegg, E.D. (1990). The classification and timing of spermatogenesis. In Histological and Histopathological Evaluation of the Testis (Cache River Press), pp. 41–58.

Russell, W.L., Kelly, E.M., Hunsicker, P.R., Bangham, J.W., Maddux, S.C., and Phipps, E.L. (1979). Specific-locus test shows ethylnitrosourea to be the most potent mutagen in the mouse. Proc. Natl. Acad. Sci. USA *76*, 5818–5819.

Schwartz, D., Goldfinger, N., Kam, Z., and Rotter, V. (1999). P53 controls low DNA damage-dependent premeiotic checkpoint and facilitates DNA repair during spermatogenesis. Cell Growth Differ. *10*, 665–675.

Silver, L.M. (1995). Reproduction and breeding. In Mouse Genetics, L.M. Silver, ed. (Oxford University Press), pp. 62–75.

Slegtenhorst-Eegdeman, K.E., de Rooij, D.G., Verhoef-Post, M., van de Kant, H.J., Bakker, C.E., Oostra, B.A., Grootegoed, J.A., and Themmen, A.P. (1998). Macroorchidism in FMR1 knockout mice is caused by increased Sertoli cell proliferation during testicular development. Endocrinology *139*, 156–162.

Smith, B.E., and Braun, R.E. (2012). Germ cell migration across Sertoli cell tight junctions. Science *338*, 798–802.

Takubo, K., Ohmura, M., Azuma, M., Nagamatsu, G., Yamada, W., Arai, F., Hirao, A., and Suda, T. (2008). Stem cell defects in ATM-deficient undifferentiated spermatogonia through DNA damage-induced cell-cycle arrest. Cell Stem Cell *2*, 170–182.

Tokuda, M., Kadokawa, Y., Kurahashi, H., and Marunouchi, T. (2007). CDH1 is a specific marker for undifferentiated spermatogonia in mouse testes. Biol. Reprod. *76*, 130–141.

Yin, Y., Stahl, B.C., DeWolf, W.C., and Morgentaler, A. (1998). p53-mediated germ cell quality control in spermatogenesis. Dev. Biol. *204*, 165–171.

Zalzali, H., Rabeh, W., Najjar, O., Abi Ammar, R., Harajly, M., and Saab, R. (2018). Interplay between p53 and Ink4c in spermatogenesis and fertility. Cell Cycle *17*, 643–651.